

Designing a Resilient Allee-Ornstein-Uhlenbeck model

Luis F. Gordillo

Department of Mathematics and Statistics, Utah State University, Logan, UT

Priscilla E. Greenwood

Department of Mathematics, University of British Columbia, Vancouver, BC

Abstract

In stochastic population dynamics, stochastic wandering can produce transition to an absorbing state. In particular, under Allee effects, low densities amplify the possibility of population collapse. We investigate this in an Allee-Ornstein-Uhlenbeck (Allee-OU) model, that couples a bistable Allee growth equation, with demographic noise, and environmental fluctuations modeled as an Ornstein-Uhlenbeck process. This process replaces the bifurcation parameter of the deterministic Allee effect equation. In the model, small noise may induce escape from the safe basin around the positive equilibrium toward extinction. We construct a stochastic control, altering the process to have a stationary distribution. We enable tractable control design, approximating the process by one with a stationary distribution. Two controlled models are developed, one acting directly on population size and another also modulating the environment. A threshold-based implementation minimizes the frequency of interventions while maximizing safe time. Simulations demonstrate that the control stabilizes fluctuations around the equilibrium.

Keywords: Resilience, Allee effect, Ornstein-Uhlenbeck process, population extinction, control strategy.

1 Introduction

In population ecology, C.S. Holling introduced the concept of resilience as referring to a population's capacity to withstand disturbances, such as environmental changes or human impact, while retaining its main functions, structure and dynamic interactions among its parts (Holling [1973]). In the face of escalating global environmental changes, resilience has become a cornerstone of conservation biology, encouraging strategies which safeguard vulnerable populations from tipping points that could lead to collapse (Walker et al. [2004]). In this paper we interpret resilience as the property of a stochastic dynamical system that its paths return near a quasi-stable state when the risk of imminent extinction has crossed a threshold. In the context of a stochastic population process, a way to quantify resilience is via the probability that the population size remains in a desired region with low risk of extinction, for a relatively long time. Here, we aim to maximize such a probability by using a control strategy.

A feature threatening ecological resilience is the Allee effect, where per capita fitness declines with decreasing population abundances due to mechanisms such as mate-finding failures, cooperative foraging, or inbreeding depression (Courchamp et al. [2008]). In the presence of strong Allee effects, characterized by positive per capita growth rates only above a critical threshold, bistable dynamics emerge with a positive stable equilibrium, while extinction serves as an absorbing state.

In conservation contexts, Allee effects complicate recovery efforts: reintroduced populations often fail if initial abundances fall short of the Allee threshold, as seen in efforts to bolster African wild dog (*Lycaon pictus*) packs, where social cooperation thresholds amplify stochastic losses (Courchamp and Macdonald [2001]). Moreover, in a changing climate, Allee effects may interact with habitat loss and pollution, pushing species toward critical slowing down, a precursor to abrupt shifts, emphasizing the need for proactive interventions to enhance resilience (Drake and Griffen [2010]).

The situations mentioned above suggest that we study the classical equation for the strong Allee effect where the bifurcation parameter is modeled as an Ornstein-Uhlenbeck process. Here we interpret ecological resilience in the context of stochastic dynamical systems as the propensity of population paths to recover to a quasi-stable state once extinction risk surpasses a predefined threshold. Resilience can be measured quantitatively by the probability that population size persists within a “safe” region for extended periods, minimizing the mean time to extinction (Grasman et al. [2005]). Our objective is to enhance this probability via a control strategy that embodies conservation interventions, e.g. supplementary feeding, translocation, or habitat augmentation, that nudge trajectories away from danger zones. By pulling paths back toward the safe equilibrium, controls emulate ecological management tactics that may extend population viability amid uncertainty.

Drawing on stochastic control theory (Mil’shtein and Ryashko [1995], Ryashko and Bashkirtseva [2008]), we derive feedback regulators that stabilize our system by relatively rare interventions, aligning with cost-effective conservation principles. The Wentzell-Friedlin theory is used to approximate the quasi-equilibrium process with a process having a true equilibrium, as other authors do (Bashkirtseva and Ryashko [2011], Ryashko and Bashkirtseva [2015], Ryashko [2018]), enabling design and computation of control even when the original system has an absorbing state. This tool has been used successfully in other applications (Bashkirtseva et al. [2015], Bashkirtseva and Ryashko [2025]) and, in particular, becomes useful in our study which includes environmental control and where full stationarity is unattainable.

The paper is structured as follows. Section 2 reviews the Allee-Ornstein-Uhlenbeck model, introducing demographic noise into the classic Allee growth equation and environmental fluctuations via an Ornstein-Uhlenbeck driven bifurcation parameter, with simulations that illustrate extinction risks. Section 3 derives a stationary law approximation and confidence ellipses to quantify safe-region persistence. In Section 4 we construct two variants of control: one acting solely on population size (mimicking direct demographic intervention) and another also modulating the parameter process (reflecting environmental engineering). Section 5 proposes an adaptive implementation strategy, activating controls threshold-wise to minimize effort while maximizing safe time. We conclude in Section 6 with ecological implications, including ties to conservation and contrasts with early-warning paradigms.

2 An Allee-Ornstein-Uhlenbeck model

The Allee effect is characterized by a positive correlation between population density and the per capita population growth rate (Courchamp et al. [2008]), for which several alternative mathematical models have been proposed. In particular for this paper, we adopt the commonly used scaled differential equation for the population density $x = x(t)$,

$$\frac{dx}{dt} = x^2(1 - x) - \rho x, \quad \rho > 0.$$

This model for the Allee effect has a saddle-node bifurcation at the critical parameter value $\rho_{\text{critical}} = 1/4$; if $\rho > 1/4$ the origin is the only stable equilibrium but if $\rho < 1/4$ two additional, non-trivial equilibria appear, one unstable and other stable. See the red parabola in Figure 1b.

We want to consider a stochastic model that has this deterministic Allee effect model as a main structure. We consider two types of stochasticity that are biologically relevant, demographic and environmental noise. Demographic noise, which refers to random fluctuations in population size due to births and deaths, is in general modeled by adding a multiplicative noise term to the population growth equation, which in our case is the Allee effect model,

$$dx = (x^2(1-x) - \rho x) dt + \sqrt{\psi x} dW, \quad (1)$$

where $\psi > 0$ and dW is a one dimensional Brownian motion (Dennis et al. [2016]).

In our approach, we incorporate environmental noise by modeling the bifurcation parameter corresponding to the equation of the Allee effect as an Ornstein-Uhlenbeck (OU) stochastic process (Gordillo and Greenwood [2024]). This differs from the common practice of letting the parameters fluctuate independently at each time point as a centered Gaussian random variable with variance that is fixed or depends quadratically on the population size, e.g. (Dennis et al. [2016]).

The drift term of an OU process pulls the parameter back toward a long-term mean, and the diffusion term adds stochasticity. This makes the OU process suitable to represent environmental factors that do not jump erratically but evolve smoothly over time. Moreover, the tendency of a stochastic parameter to revert to a stable mean is ideal for modeling cases where significant deviations are temporary and the environment tends to stabilize around a typical state. Thus $\rho = \rho(t)$ is now a solution of the stochastic differential equation

$$d\rho = -\lambda(\rho - \rho_{\text{center}})dt + \phi dW, \quad (2)$$

with $\lambda, \phi > 0$ fixed. One characteristic of the process ρ is that its paths fluctuate about ρ_{center} with a tendency of moving towards ρ_{center} that is regulated by λ . In practice, this might describe how environmental factors exhibit temporary deviations from its mean but return to it over time. In contrast to Brownian motion, the OU process avoids unbounded growth or decline, making it a reasonable model for external fluctuations.

Our Allee-OU model is obtained by coupling the Allee effect equation with demographic noise (1) with the OU equation (2),

$$d\mathbf{X}_t = F(\mathbf{X}_t)dt + \epsilon \sigma(\mathbf{X}_t)d\mathbf{W}_t, \quad \epsilon > 0, \quad (3)$$

where

$$\mathbf{X}_t = \begin{bmatrix} x(t) \\ \rho(t) \end{bmatrix} = \begin{bmatrix} x \\ \rho \end{bmatrix}, \quad F(\mathbf{X}_t) = \begin{bmatrix} x^2(1-x) - \rho x \\ -\lambda(\rho - \rho_{\text{center}}) \end{bmatrix}, \quad \sigma(\mathbf{X}_t) = \begin{bmatrix} \sqrt{\psi x} & 0 \\ 0 & \phi \end{bmatrix}$$

and $d\mathbf{W}_t$ is a two dimensional Brownian motion.

2.1 Behavior of the field $F(\mathbf{X})$

In what follows, let $\mathbf{X} = [x \ \rho]'$ denote a column vector of coordinates in the phase-plane. We begin by describing the behavior of equation (3) in the deterministic case, i.e. $\epsilon = 0$, with $\rho_{\text{center}} < \rho_{\text{critical}}$. Our focus is on the regime where ρ_{center} is sufficiently close to ρ_{critical} that even small positive values of ϵ can produce phase transitions in the system's dynamics.

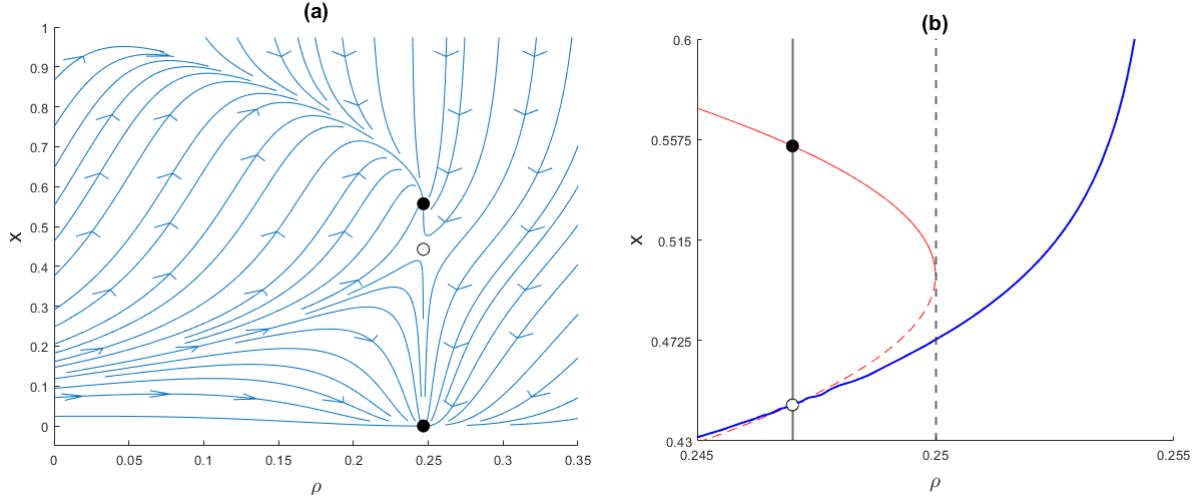


Figure 1: (a) Phase portrait for the equation $d\mathbf{X}/dt = F(\mathbf{X})$, with $\lambda = 0.097$ and $\rho_{center} = 0.247$. Equilibria are marked with a black (stable) and open (unstable) circles. (b) Positive equilibria and isoclines of the components of $d\mathbf{X}/dt = F(\mathbf{X})$ (red parabola and grey continuous vertical line) for $\lambda = 0.01$ and $\rho_{center} = 0.247$. The basin of attraction of the stable equilibrium is determined by the separatrix emerging from the unstable equilibrium (solid blue).

The differential equation $d\mathbf{X}/dt = F(\mathbf{X})$ has three equilibria. The first, $[0 \ \rho_{center}]'$, which is stable, and two more, denoted by \mathbf{X}_u^* and \mathbf{X}_s^* , which are unstable and stable, respectively, see Figure 1(a). Figure 1(b) shows the isoclines, determined by $F(\mathbf{X}) = 0$, as the parabola in red and the vertical continuous gray line. The separatrix of the system, which determines the basins of attraction of the stable equilibria, is the blue curve. Notice the region to the right of the vertical line at $\rho_{critical} = 0.25$ that is contained in the basin of attraction of \mathbf{X}_s^* .

2.2 Simulations of model (3)

Two sample paths of the process \mathbf{X}_t are shown in Figure 2. The maximum number of time steps for the simulations is 4×10^4 , with parameters as in Figure 1(b), $\lambda = 0.01$, $\rho_{center} = 0.247$, $\phi = 0.04$, $\psi = 0.1$ and $\epsilon = 0.005$. In each panel, the path begins at \mathbf{X}_s^* . In (a), the path briefly crosses the separatrix but then returns to fluctuate near \mathbf{X}_s^* . In (b), after crossing the separatrix, the path is drawn toward the equilibrium on the horizontal axis, corresponding to the extinction of the population. The Figure indicates that the paths spend most of the time in a neighborhood of the stable equilibrium and suggests one might design a control to prevent extinction. The histogram in Figure 3 approximates the conditional probability distribution of the time to extinction given a fixed computational time, using the first crossing of the level $x = 0.4$ as a proxy. Among 5000 simulated paths, 2630 ended in extinction.

3 Approximation by a model with stationary law

In many papers, the study of a system like (3) is done via the corresponding Fokker-Planck equation. When this equation is set equal to zero its solution is the stationary law. This is done with the hope that the answer to the question asked will not change very much, if it makes sense at all,

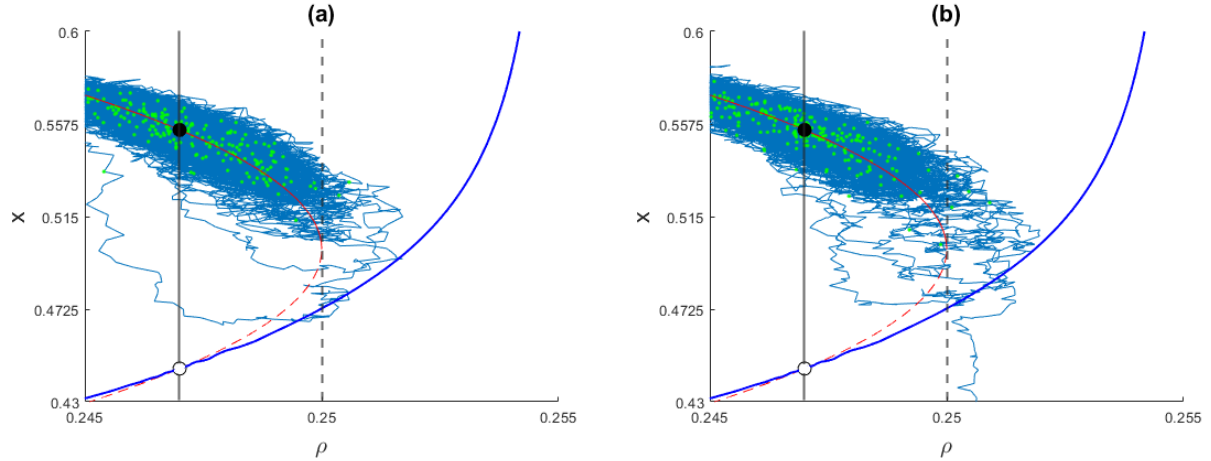


Figure 2: Sample paths of the process \mathbf{X}_t starting at the stable equilibrium \mathbf{X}_s^* , with parameters $\lambda = 0.01$, $\rho_{\text{center}} = 0.247$, $\phi = 0.04$, $\psi = 0.1$ and $\epsilon = 0.005$. Green dots along the paths are time markers at each 150 time steps, indicating where the path lingers most of the time.

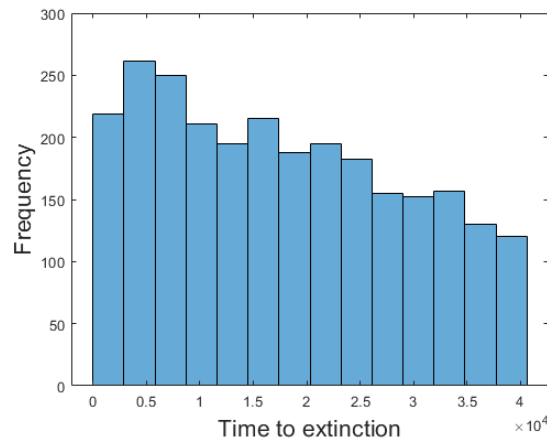


Figure 3: Histogram of times to extinction given a fixed computational duration of 4×10^4 time steps. Extinction time is approximated by the first crossing of the level $x = 0.4$. As illustrated in Figure 2, sample paths may cross the separatrix and subsequently be attracted to the equilibrium $[0 \ \rho_{\text{center}}]'$, corresponding to population extinction. The parameters used are the same as in Figure 2.

and because computations are usually easier in the context of the stationary process. Here we are interested in computing a control which, applied to our model (3), will cause it to be resilient against the variable environment, represented in our model by regarding the parameter ρ as an OU process. We follow a line of development of Ryashko and Bashkirtseva [2008, 2015] using the stationary approximation and accompanying confidence ellipses to compute controls, which we then introduce into our system (3) to create resilience.

For small $\epsilon > 0$, the stationary distribution $p = p(\mathbf{X}, \epsilon)$ concentrated around \mathbf{X}_s^* satisfies

$$-\nabla \cdot F(\mathbf{X})p + \frac{\epsilon^2}{2} \left[\frac{\partial^2}{\partial x^2} S_{11}(\mathbf{X})p + \frac{\partial^2}{\partial \rho^2} S_{22}(\mathbf{X})p \right] = 0, \quad (4)$$

where $S_{11}(\mathbf{X})$ and $S_{22}(\mathbf{X})$ are the elements of the diagonal in $S(\mathbf{X}) = \sigma(\mathbf{X})\sigma(\mathbf{X})'$, the apostrophe denoting the transpose. The law of the process satisfying (3) is quasi-stationary, i.e. the probability slowly leaks across the separatrix towards the horizontal axis. For small ϵ we can use the approximation of order $O(1/\epsilon^2)$

$$p(\mathbf{X}, \epsilon) \approx M \exp \left[-\frac{Q(\mathbf{X})}{\epsilon^2} \right], \quad (5)$$

where M is a normalization constant (E et al. [2019], Freidlin and Wentzell [1998]) and $Q(\mathbf{X})$ can be approximated by

$$Q(\mathbf{X}) \approx \frac{1}{2}(\mathbf{X} - \mathbf{X}_s^*)'W^{-1}(\mathbf{X} - \mathbf{X}_s^*), \quad (6)$$

where W^{-1} is a positive definite matrix and with an error of order $|\mathbf{X} - \mathbf{X}_s^*|^3$ (Mil'shtein and Ryashko [1995]). As shown there, the matrix W satisfies

$$JW + WJ' + S = 0, \quad (7)$$

where for us J is the Jacobian of the function F in (3),

$$J = \begin{pmatrix} 2x - 3x^2 - \rho & -x \\ 0 & -\lambda \end{pmatrix}, \quad (8)$$

evaluated at

$$\mathbf{X}_s^* = \left(\frac{1}{2} \left(1 + \sqrt{1 - 4\rho_{\text{center}}} \right), \rho_{\text{center}} \right)'$$

and $S = S(\mathbf{X}_s^*) = \sigma(\mathbf{X}_s^*)\sigma(\mathbf{X}_s^*)'$. We combine (5) and (6) to approximate $p(\mathbf{X}, \epsilon)$ as a Gaussian with covariance $\epsilon^2 W$,

$$p(\mathbf{X}, \epsilon) \approx M \exp \left[-\frac{(\mathbf{X} - \mathbf{X}_s^*)'W^{-1}(\mathbf{X} - \mathbf{X}_s^*)}{2\epsilon^2} \right], \quad (9)$$

when ϵ is small and during time intervals where \mathbf{X} is close to \mathbf{X}_s^* .

With the parameters chosen for our simulations in Section 2.3, the matrix W is computed by solving equation (7),

$$W = \begin{bmatrix} 6.1811 & -0.6271 \\ -0.6271 & 0.08 \end{bmatrix}.$$

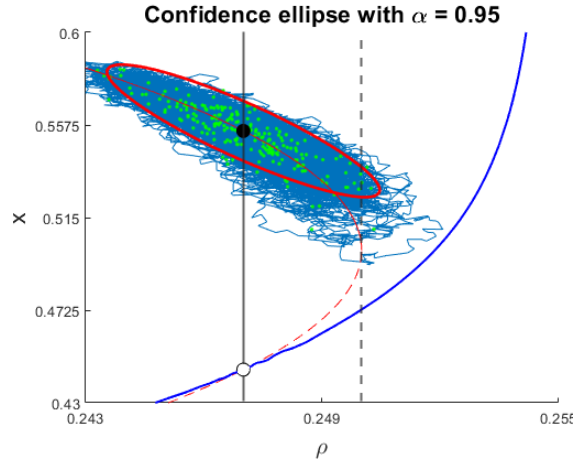


Figure 4: Confidence ellipse for the approximate model with stationary law and level of confidence $\alpha = 0.95$ plotted together with a sample path of the process \mathbf{X}_t , solution of equation (3), with $\mathbf{X}_0 = \mathbf{X}_s^*$ and time horizon T . Our impression from the plot is that the approximating stationary law is a reasonable proxy for the law of the process \mathbf{X}_t within the chosen T . Parameters for the process are the same as in Figure 2.

We use the matrix W to construct confidence ellipses centered at \mathbf{X}_s^* . These ellipses delineate the regions in which the values of the approximate process with stationary law are concentrated. For a fixed $\epsilon > 0$, a confidence ellipse is defined by the quadratic

$$(\mathbf{X} - \mathbf{X}_s^*)' W^{-1} (\mathbf{X} - \mathbf{X}_s^*) = 2\epsilon^2 q, \quad q > 0, \quad (10)$$

where q is a chi-squared value, $q = -\ln(1 - \alpha)$, α being the level of desired confidence (e.g. 95%) for the values under the stationary process. See the Appendix in (Greenwood and Nikulin [1996]) or (Johnson and Wichern [2007]) Chapter 4. In other words, α is the probability that a value of the process under the law $p(\mathbf{X}, \epsilon)$ will be inside the ellipse, Figure 4. The ellipse's semi-axes are scaled by the square roots of W 's eigenvalues, with orientations given by its eigenvectors, centered at \mathbf{X}_s^* . As shown in Figure 4, paths of the process \mathbf{X}_t , solution of the system (3), can make excursions outside the ellipse. During some of those excursions, a path might cross the separatrix and be subsequently drawn toward $[0 \ \rho_{\text{center}}]'$.

4 Control of the stochastic system

When ϵ is small, sample paths of system (3) fluctuate for some time near the nontrivial equilibrium \mathbf{X}_s^* . However, they eventually exit its basin of attraction, crossing the separatrix, as seen in Figure 2. The crossing may be followed by either a return to the basin of attraction of \mathbf{X}_s^* , as in Figure 2(a), or by being pulled to extinction by the stable equilibrium $[0 \ \rho_{\text{center}}]'$, Figure 2(b). How can the system (3) be stabilized, that is, modified in real time to sustain fluctuations near \mathbf{X}_s^* and prevent extinction? and can we design a strategy such that the control is used only occasionally, only when needed? As in (Ryashko and Bashkirtseva [2015], Ryashko [2018]), our modifications rely on observations of the current time values of x and ρ . Let K be a 2×2 real matrix and denote explicitly the components of the stable equilibrium as $\mathbf{X}_s^* = [x^* \ \rho^*]'$. Then introduce a control

function, U , a feedback regulator, defined as

$$U(\mathbf{X}) = \begin{bmatrix} u_1(\mathbf{X}) \\ u_2(\mathbf{X}) \end{bmatrix} = K(\mathbf{X} - \mathbf{X}_s^*) = \begin{bmatrix} k_{11} & k_{12} \\ k_{21} & k_{22} \end{bmatrix} \begin{bmatrix} x - x^* \\ \rho - \rho^* \end{bmatrix}, \quad (11)$$

into the main equation (3),

$$d \begin{bmatrix} x \\ \rho \end{bmatrix} = \underbrace{\left(\begin{bmatrix} x^2(1-x) - \rho x \\ -\lambda(\rho - \rho_{\text{center}}) \end{bmatrix} + \begin{bmatrix} k_{11} & k_{12} \\ k_{21} & k_{22} \end{bmatrix} \begin{bmatrix} x - x^* \\ \rho - \rho^* \end{bmatrix} \right)}_{G(\mathbf{X}, U) := F(\mathbf{X}) + U(\mathbf{X})} dt + \epsilon \begin{bmatrix} \sqrt{\psi x} & 0 \\ 0 & \phi \end{bmatrix} \begin{bmatrix} dW_1 \\ dW_2 \end{bmatrix}. \quad (12)$$

Let us denote the new drift function by G . Notice that, although the system has changed, the point \mathbf{X}_s^* is still an equilibrium for the new drift. We want \mathbf{X}_s^* to be stable, so the sample paths of the process \mathbf{X}_t keep fluctuating around it. This can be achieved if the matrix K belongs to the set

$$\mathbb{K} = \{K \mid \text{the real parts of the eigenvalues of } J + BK \text{ are negative}\}, \quad (13)$$

where $B = \partial G / \partial U(\mathbf{X}_s^*, 0)$, is the Jacobian of the control with respect to U evaluated at $(\mathbf{X}_s^*, 0)$, (Ryashko and Bashkirtseva [2008]). We examine two scenarios: (1) the control influences both the population x and the process ρ , and (2) the control influences only the population x . These correspond to distinct kinds of environment: the former represents controlled settings, such as a laboratory, while the latter reflects broader, uncontrolled scenarios, like natural environments.

4.1 U acts on x and ρ

Let us construct a control U that acts on both components of \mathbf{X}_t , that is, the $\text{rank}(B)$ is equal to 2. Following (Ryashko and Bashkirtseva [2008]), the new stochastic sensitivity matrix W is a solution of the equation

$$(J + BK)W + W(J + BK)' + S = 0, \quad (14)$$

which is analogous to equation (7) obtained for the system without control. The matrix K can be computed as

$$K = -B^{-1} \left(J + \frac{1}{2} SW^{-1} \right). \quad (15)$$

In our case, B is the identity matrix I . As explained in (Ryashko and Bashkirtseva [2008]), the matrix W can be chosen as a multiple of the identity, wI , with w small, which results in a matrix K that belongs to \mathbb{K} . For our example we chose $w = 0.04$, which yields the matrices

$$W = \begin{bmatrix} 0.04 & 0 \\ 0 & 0.04 \end{bmatrix}, \quad K = \begin{bmatrix} -0.6271 & 0.5548 \\ 0 & -0.01 \end{bmatrix}.$$

Figure 5(a) shows a path of the controlled process, solution of (12), that starts at \mathbf{X}_s^* , computed for the time horizon T . We see that the path fluctuates very close around the equilibrium. A confidence ellipse under the approximate stationary law for the controlled process appears in red.

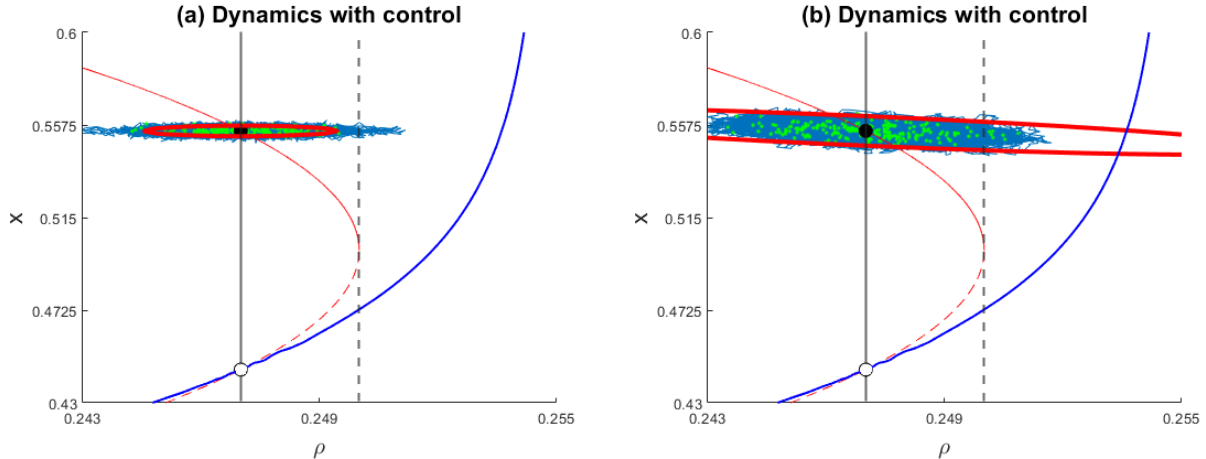


Figure 5: Sample paths of the system (12) with control U starting at \mathbf{X}_s^* and plotted on top of Figure 1(b) only for reference. Confidence ellipses under the approximate stationary law for the controlled process are the thick red curves. (a) U acts on x and ρ . (b) U acts only on x . Contrasting with Figure 4, the controlled paths are kept tightly close to the stable equilibrium \mathbf{X}_s^* in both cases. All the parameters and the level of confidence, α , are as in Figure 4.

4.2 U acts only on x

Let us construct a control U that acts only on x , i.e. $k_{21} = k_{22} = 0$ in (11), which makes $\text{rank}(B)$ equal to one. Let us write

$$H(W) = JW + WJ' + S,$$

then, following (Ryashko and Bashkirtseva [2008]), the matrix W must satisfy

$$PH(W)P = 0, \quad (16)$$

where $P = I - BB^+$ and B^+ is the pseudoinverse of B . It is also shown there that the matrix K can be computed using the formula

$$K = -\frac{1}{2}B^+H(W)(P + I)W^{-1}. \quad (17)$$

The diagonal entries of the matrix W may be assigned a common value $w > 0$, provided that the condition in (13) is satisfied. The computations also show that the elements off the diagonal of W coincide with those in the matrix corresponding to the uncontrolled system. In view of the constraints, for our example, a possible way of defining the matrix W and the corresponding matrix K are

$$W = \begin{bmatrix} 0.8 & -0.6271 \\ -0.6271 & 0.8 \end{bmatrix}, \quad K = \begin{bmatrix} -0.0451 & 0.4639 \\ 0 & 0 \end{bmatrix}.$$

Figure 5(b) shows a path of the controlled process, solution of (12), that starts at \mathbf{X}_s^* , computed for the time horizon T . We see that the path fluctuates very close around the equilibrium. A confidence ellipse under the approximate stationary law for the controlled process appears in red.

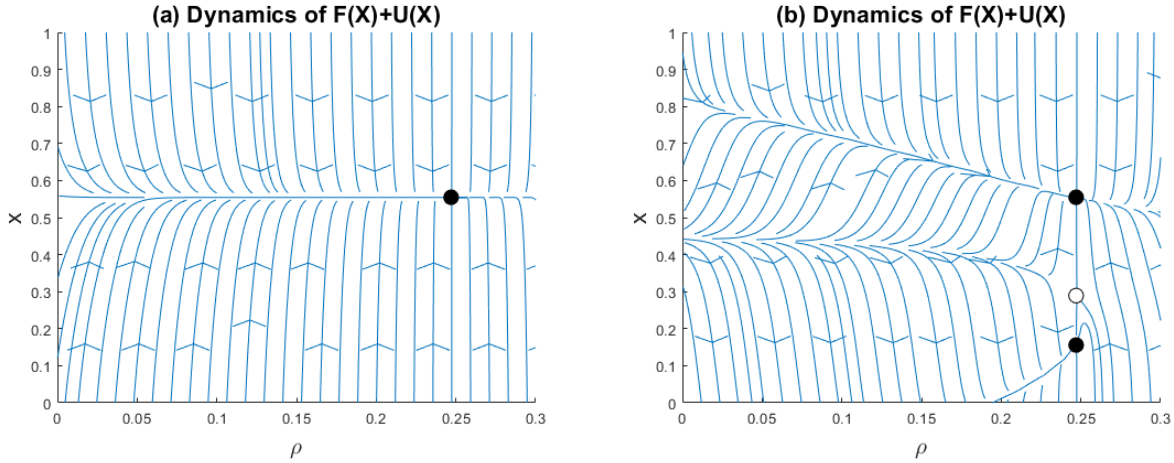


Figure 6: Phase portrait for the equation $d\mathbf{X}/dt = F(\mathbf{X}) + U(\mathbf{X})$, with parameters $\lambda = 0.01$ and $\rho_{\text{center}} = 0.247$. (a) The matrix K is computed as indicated in Section 4.1. (b) The matrix K is computed as indicated in Section 4.2.

4.3 Dynamics under the controlled field $F(\mathbf{X}) + U(\mathbf{X})$

It is straightforward to verify that the point \mathbf{X}_s^* , the stable equilibrium of the field without control, is also a stable equilibrium of $d\mathbf{X}/dt = F(\mathbf{X}) + U(\mathbf{X})$. However, other equilibria are different. In our example, the system controlling both variables as indicated in Section 4.1 has only one real, stable equilibrium, Figure 6(a), whereas when controlling only x according to Section 4.2, the system has two positive stable and one unstable equilibria, Figure 6(b). Although in both cases stochasticity will eventually cause any path that starts close to \mathbf{X}_s^* to move against the deterministic flow and to hit the horizontal axis with probability one, the time for this to happen is relatively large in comparison with that of the model without the control. For instance, we repeated 5000 simulations for each type of control and in none of them did the path reach extinction during the same time frame used for generating the histogram in Figure 3.

5 A strategy for implementing the control

Our proposed strategy combines the controlled and uncontrolled processes, creating a new process with a stationary law, centered around \mathbf{X}_s^* . Paths of the new process will fluctuate near \mathbf{X}_s^* with high probability. The idea is to replace the uncontrolled process with the controlled one whenever the risk of extinction becomes high, thereby driving the system back to a neighborhood of \mathbf{X}_s^* . Once the trajectory is near this equilibrium, the dynamics switches back to the uncontrolled process, creating an alternating pattern. Figure 7 shows a schematic of the procedure, where the control is implemented when the path of the population process crosses a fixed level. This procedure creates a stationary process. The next aim would be to maximize the time spent near \mathbf{X}_s^* and minimize the use of the control.

The criteria chosen to activate the control would depend on the cost of implementing the system (12). Let us consider the cost of the control as described in Section 4.2, that is, with U acting only on the population process x . Figure 8(a) shows a path of such a controlled process starting at an arbitrary point on the line defined by $x = 0.432$, with ρ between 0.243 and 0.255, which quickly

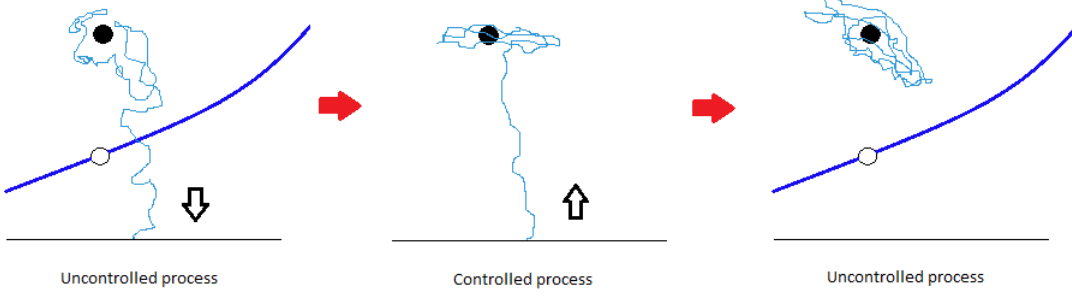


Figure 7: Strategy for implementing the control. **Left:** A path of the uncontrolled process fluctuates around \mathbf{X}_s^* (black dot). It eventually crosses the separatrix (blue curve) and is pulled down until it meets a predetermined horizontal level (horizontal black line). **Center:** The controlled process activates, drawing the path upward toward the equilibrium \mathbf{X}_s^* , where it fluctuates for a short time. **Right:** Switch back to the uncontrolled process.

stabilizes around \mathbf{X}_s^* . We call this point the “initial point of return”. The control in this case is

$$U(\mathbf{X}_t) = \begin{bmatrix} u_1(\mathbf{X}_t) \\ 0 \end{bmatrix}, \quad u_1(\mathbf{X}_t) = k_{11}(x - x^*) + k_{12}(\rho - \rho_{\text{center}}).$$

In classical stochastic control theory (e.g., Fleming and Rishel [1975]), the cost of implementing a feedback control $U(\mathbf{X}_t)$ is quantified through an expected infinite-horizon quadratic cost functional. This functional penalizes deviations of the state variables, i.e. cost of stabilizing the system near the equilibrium, and the effort required to apply the control. We set our control cost C considering only penalties of the former type. We define C as

$$C = \mathbb{E} \left[\int_0^\tau r [k_{11}(x - x^*) + k_{12}(\rho - \rho_{\text{center}})]^2 dt \right], \quad (18)$$

where $r > 0$ is the relative penalty for the control u_1 and τ is the returning time (first passage time) from the initial point of return through the barrier defined by $x = x^* - \eta$, $\eta > 0$ small. The choice of η must ensure that, with high probability, beyond this boundary the path resumes fluctuating around \mathbf{X}_s^* when the control is removed.

The cost function is based on deviations of $x(t)$ from x^* and $\rho(t)$ from ρ_{center} . The term $k_{12}(\rho - \rho_{\text{center}})$ is the cost for responding to environmental fluctuations. Figure 8(b) shows the control cost, C , of moving the process from the initial point of return to the first crossing of the horizontal line $x = x^* - 0.005$. For each value of ϵ , the cost C is estimated as the average of 300 simulations, with $r = 1$, and the initial point of return, as stated before, with $x(0)$ on the line defined by $x = 0.432$ and ρ_0 drawn uniformly in $[0.235, 0.255]$. The plot shows that the control cost C barely increases with increasing ϵ but its variability increases.

Figure 8(c) shows the mean of the return time τ (first passage time) through the boundary $x = x^* - 0.005$, which slightly decreases with increasing ϵ , whereas its variability increases.

6 Conclusions and discussion

In this paper we propose a way to construct resilience in stochastic population models exhibiting Allee effects. We use a stationary distribution approximation to derive a strategy that ideally

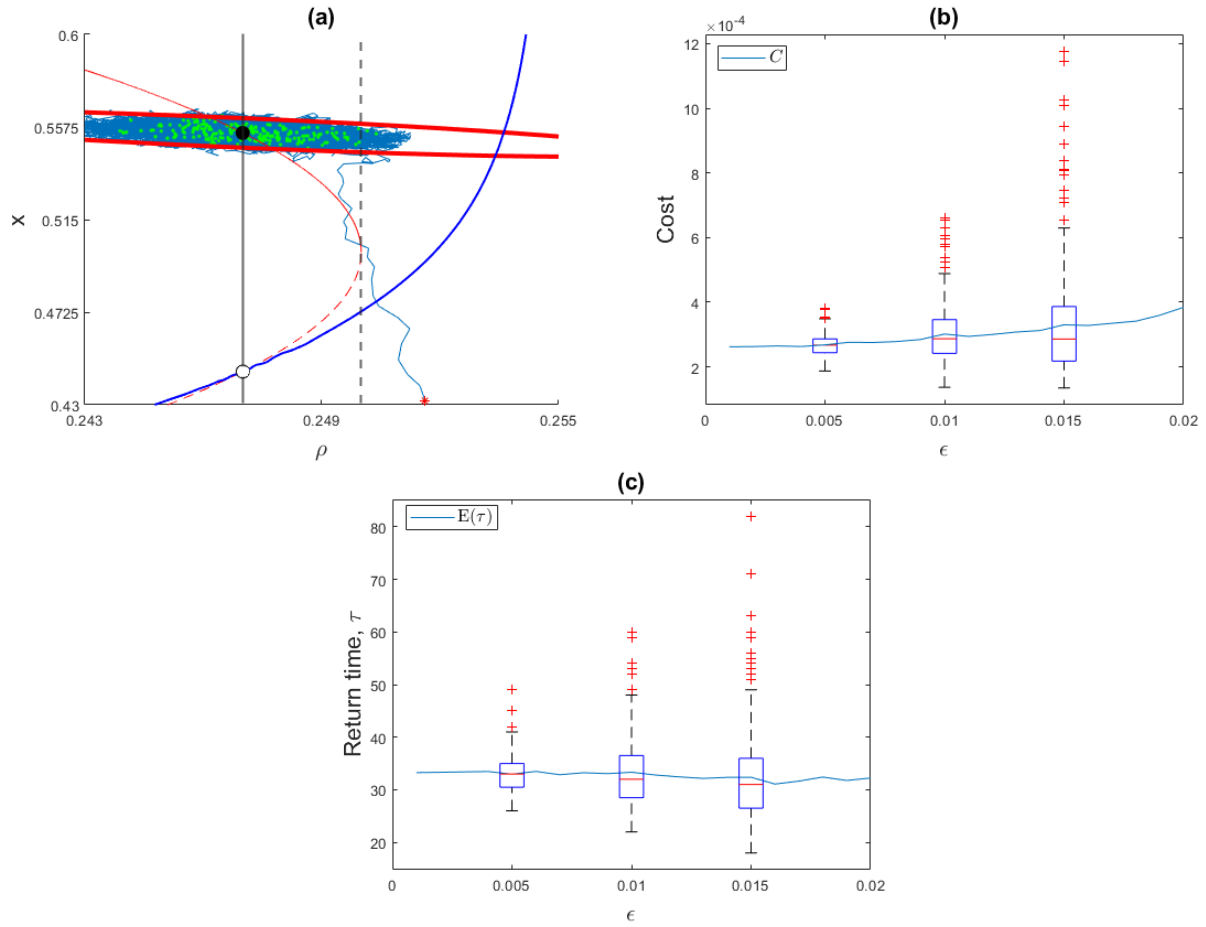


Figure 8: (a) A path of the controlled process representing the intermediate stage of the extinction-avoidance strategy illustrated in Figure 7. (b) The control cost and boxplots, as function of ϵ . (c) Mean and boxplots of the return time τ (first passage time) through the boundary $x = x^* - 0.005$.

eliminates extinction risks. The novelty here is the computation of controls for the Allee-OU model. Our simulations reveal that these controls can largely confine fluctuations of the process around the safe equilibrium \mathbf{X}_s^* , reducing extinction probabilities from over 50% in uncontrolled paths to near zero in controlled regimes over a simulated time horizon.

Although we do not address the problem of how to execute the control, our control design offers a theoretical tool for proactive conservation in Allee-afflicted species, where low densities may precipitate failures in fitness components such as mating or foraging cooperation. The control executed only on the population (U acting only on x) suggests direct interventions such as supplementary feeding or translocations, which artificially increase the density toward a safe region. In contrast, the dual control (U acting on both x and ρ), echoes environmental engineering tactics, such as habitat restoration or targeted predator removal to revert fluctuations toward favorable states. Our threshold-activated implementation triggers interventions only when paths cross a predefined risk boundary. Our simulations show that the time spent by the process around the equilibrium \mathbf{X}_s^* between the applications of the control is large in comparison to the time spent under the control, see Figures 3 and 8(c).

Our two-dimensional, non-spatial model does not include the effects of dispersal among population patches, which might induce secondary effects, such as “emergent resilience”. This refers to the possibility of dispersal acting as a stabilizing force by importing individuals from other source patches, countering local extinctions, a “rescue effect”. This can make the overall metapopulation more robust to noise than isolated patches would suggest.

Our approach of dynamic stabilization contrasts with early-warning signals that detect imminent collapses via precursors such as increased variance or autocorrelation (Drake and Griffen [2010]). While early-warning signals excel in forecasting demographic regime shifts, our controls prevent such transitions by reshaping the stochastic dynamics landscape.

Future extensions could incorporate spatial heterogeneity and multi-species interactions, e.g., predator-prey Allee cascades. We hope that our construction contributes to the transformation of theoretical resilience understanding to actionable conservation.

Data availability. MATLAB codes used to generate the figures are available at <https://github.com/LuisFGordillo/Codes>

References

- I. Bashkirtseva and L. Ryashko. Positive and negative role of random perturbations in the dynamics of a tumor-immune system with treatment. *Journal of Mathematical Biology*, 91(2):20, 2025. doi: 10.1007/s00285-025-01694-y.
- I. Bashkirtseva and L.B. Ryashko. Sensitivity analysis of stochastic attractors and noise-induced transitions for population model with Allee effect. *Chaos*, 21(4):047514, 2011. doi: 10.1063/1.3647316.
- I. Bashkirtseva, A.B. Neiman, and L.B. Ryashko. Stochastic sensitivity analysis of noise-induced suppression of firing and giant variability of spiking in a Hodgkin–Huxley neuron model. *Physical Review E*, 91(5):052920, 2015. doi: 10.1103/PhysRevE.91.052920. URL <https://doi.org/10.1103/PhysRevE.91.052920>.

F. Courchamp and D.W. Macdonald. Crucial importance of pack size in the african wild dog *lycaon pictus*. *Animal Conservation*, 4:169–174, 2001.

F. Courchamp, L. Berec, and J. Gascoigne. *Allee Effects in Ecology and Conservation*. Oxford Biology. Oxford University Press, Oxford; New York, 2008. ISBN 9780198570301. doi: 10.1093/acprof:oso/9780198570301.001.0001.

B. Dennis, L. Assas, S. Elaydi, E. Kwessi, and G. Livadiotis. Allee effects and resilience in stochastic populations. *Theoretical Ecology*, 9(3):323–335, 2016. doi: 10.1007/s12080-015-0288-2.

J.M. Drake and B.D. Griffen. Early warning signals of extinction in deteriorating environments. *Nature*, 467(7314):456–459, 2010. doi: 10.1038/nature09389.

W. E, T. Li, and E. Vanden-Eijnden. *Applied Stochastic Analysis*, volume 199 of *Graduate Studies in Mathematics*. American Mathematical Society, Providence, RI, 2019. ISBN 978-1-4704-6569-8.

W.H. Fleming and R.W. Rishel. *Deterministic and Stochastic Optimal Control*. Springer-Verlag, Berlin, Heidelberg, 1975. ISBN 978-3-642-10944-8. doi: 10.1007/978-3-642-10942-4.

M.I. Freidlin and A.D. Wentzell. *Random Perturbations of Dynamical Systems*, volume 260 of *Grundlehren der Mathematischen Wissenschaften*. Springer, New York, NY, 2 edition, 1998. ISBN 978-3-540-90858-6.

L.F. Gordillo and P.E. Greenwood. A stochastic mechanism causing long or short transients near a bifurcation point. *Proceedings of the Royal Society A*, 480(20240329), 2024. doi: 10.1098/rspa.2024.0329.

J. Grasman, O.A. van Herwaarden, and T.H.J. Hagenaars. *Resilience and persistence in the context of stochastic population models*, pages 267–280. Springer, 2005. ISBN 9781402029011. doi: 10.1007/1-4020-2904-7_10.

P.E. Greenwood and M.S. Nikulin. *A Guide to Chi-Squared Testing*. Wiley Series in Probability and Statistics. John Wiley & Sons, New York, 1996. ISBN 0-471-55779-X, 978-0471557791.

C.S. Holling. Resilience and stability of ecological systems. *Annual Review of Ecology and Systematics*, 4:1–23, 1973. doi: 10.1146/annurev.es.04.110173.0000245.

R.A. Johnson and D.W. Wichern. *Applied Multivariate Statistical Analysis*. Pearson Prentice Hall, Upper Saddle River, NJ, 6th edition, 2007. ISBN 9780131877153.

G.N. Mil'shtein and L.B. Ryashko. A first approximation of the quasipotential in problems of the stability of systems with random non-degenerate perturbations. *Journal of Applied Mathematics and Mechanics*, 59(1):47–56, 1995. doi: 10.1016/0021-8928(95)00006-B.

L. Ryashko. Stochastic control in the problem of preventing ecological catastrophes. *IFAC-PapersOnLine*, 32(51):540–544, 2018. doi: 10.1016/j.ifacol.2018.11.478.

L. Ryashko and I. Bashkirtseva. Stochastic sensitivity analysis and control for ecological model with the Allee effect. *Mathematical Modelling of Natural Phenomena*, 10(2):130–140, 2015. doi: 10.1051/mmnp/201510209.

L.B. Ryashko and I.A. Bashkirtseva. On control of stochastic sensitivity. *Automation and Remote Control*, 69(7):1171–1180, 2008. doi: 10.1134/S0005117908070084.

B. Walker, C.S. Holling, S.R. Carpenter, and A. Kinzig. Resilience, adaptability and transformability in social-ecological systems. *Ecology and Society*, 9(2):5, 2004. URL <http://www.ecologyandsociety.org/vol9/iss2/art5>.